Assessment of the Simultaneity Factor Between PV Production and Electric Demand in a Real Scholar Canteen Belonging to a REC Through TRNSYS Simulations

Daniela Cirone – University of Calabria, Italy – Daniela.cirone@unical.it
Roberto Bruno – University of Calabria – roberto.bruno@unical.it
Piero Bevilacqua – University of Calabria, Italy – piero.bevilacqua@unical.it
Stefania Perrella – University of Calabria, Italy – stefania.perrella@unical.it
Natale Arcuri – University of Calabria, Italy – natale.arcuri@unical.it

Abstract

Solutions conceived to mitigate the mismatching between electricity production and demand in buildings are decisive in maximizing the benefits of Renewable Energy Communities. In this context, Building Energy Simulation (BES) tools can be used for accurately assessing energy flows considering variable conditions, especially if equipped with electric generation systems for heating and cooling. In this paper, a PV generator for a scholastic canteen belonging to a municipal REC, in which the main electric load is represented by a VRF heat pump, is evaluated by TRNSYS simulation to optimize the self-consumption share. A monitoring campaign targeted at the collection of real electrical profiles and climatic data was carried out to validate the building-plant model. A simultaneity factor (SF) between electric demand and production was introduced to evaluate actual self-consumption and electric surplus to share within the REC. Results showed the decisive role of Demand Side Management, whereas monocrystalline cells perform better than other technologies avoiding installing the maximum installable PV peak power. For the considered case study, despite the building being occupied occasionally, an SF of about 75% can be achieved.

1. Introduction

The reduction of CO_2 emissions and the contrast to climate change increasingly involve the existing building stock (UN Environmental Program, 2024). In this sector, to support the transition from fossil fuels to renewable sources, an appealing concept is represented by the Renewable Energy Community (REC), regulaed by the European law "Renewable Energy Directive Recast 2018/2001". The main goal of the REC implementation is the provision of environmental, economic and social community benefits by sharing produced powers in local areas. Indeed, RECs allow anyone to cooperate in the management of energy fluxes, while preserving subjective rights and duties, considering the proximity between production and consumption sites. Considering the multitude of difficult objectives, RECs are increasingly under investigation in the relevant literature. For instance, (Heuninckx et al., 2022) identified the motivations for joining a REC evaluating different stakeholders, as well as the elements to consider in the design phase involving social, economic, technical and environmental aspects. The opportunity to extend the "zero-energy building" concept at the neighborhood scale was investigated in (Marique et al., 2014) taking into account the impact of urban form on energy needs, on-site production and the energy transportation system. The choice of how a REC must be planned mainly depends on the size and building typology and the local climate, which is also decisive in assessing the renewable production. In this context, among the different available technologies to generate electric power, photovoltaics are even more contemplated in light of the favourable installation costs (Franzoi et al., 2021), as confirmed by case studies of RECs carried out in Belgium, Spain, the Netherlands, and Greece (Lode et al., 2022). On the other hand, technical challenges such as energy cost reduction and grid stability are significant parameters to take into account for the

Part of
Pernigotto, G., Ballarini, I., Patuzzi, F., Prada, A., Corrado, V., & Gasparella, A. (Eds.). 2025. Building simulation applications BSA 2024. bu,press.
https://doi.org/10.13124/9788860462022

correct system design. Grid stability can be enhanced by involving buildings with a high share of self-consumed power production, especially when characterized by particular occupation patterns. "Moreover, the share of self-consumed energy also impacts the profitability of RECs, as financial incentives are determined based on this rate. In light of this, the study is targeted to properly size a PV generator foreseen in a school canteen located in the mountain town of Soveria Mannelli (South Italy, 39°05′°N, 16°22′E) to maximize the self-consumed electric power considering different parameters such as the generator size, the cell's technology and the Demand Side Management (DSM) for matching electric production and consumption (Arcuri et al., 2018). These profiles were determined through a parametric study carried out in the TRNSYS environment to quantify the self-consumed rate using a simultaneity factor between demand and production (VV.AA., 2018). The building-plant model was validated by monitoring electric consumption and using real climatic data for a period of one month,calculating the Root Mean Square Error (RMSE) between simulated and acquired values. The use of real climatic data allowed for determining the building's thermal energy requirements and the electric consumption being the main electric load represented by a VRF heat pump for heating applications. PV size was managed by varying the array number and considering the available roof surface for installation. Regarding the PV technology, three commercial products with diverse power temperature coefficients were simulated to consider the thermal drift effect on the power output (Bevilacqua et al., 2020). The electric consumption profiles were varied by shifting the operation hours of the main electric loads. The case study building was chosen for the particular occupation pattern, being persons concentrated mainly for a few hours of the day and only for three days per week, making the meeting between production and consumption difficult. Considering that the location is characterized by a severe winter climate with particular socio-economic features, since the site is classified as a disadvantaged and isolated area, the REC implementation represents a pragmatic solution to promote social and economic development, assuming renewable technologies are properly designed to favour correct management of the energy fluxes inside the community, confirming BES suitable tools to achieve this goal.

2. Methodology

2.1 Building-Plant Description

The interaction between the building fabric, the heating plant components and the PV generators was simulated by TRNSYS 18 using climatic data of the considered site. The single-story building, whose intended use is as a school canteen, was simulated as a single thermal zone geometrically implemented by the TRNSYS3d plug-in (Fig. 1a). It is characterized by a regular rectangular shape made of hollowed external walls equipped with 5 cm of air-gap (see Table 1), not insulated because it was built before the promulgation of national laws concerning the energy consumption limitation. The opaque envelope is completed by a ground floor (Table 2) and an unheated attic separated from the heated environment by an inter-floor concrete deck. The roof (Table 3) is made of a double pitch of concrete and tiles, with approximately 15 degrees of slope, and is oriented North-East (for 200 m²) and South-West (150 m²), with the latter considered for the PV installation. The gross floor area is about 330 m² with an inter-floor height of 3.4 m. Windows are aluminium framed mounting clear double panes and equipped with PVC screens. The envelope is not shaded by fixed external obstructions. The thermal energy requirements are quite significant because the building is crumbling (see Fig. 1b). Since heating is provided by a VRF air-air heat pump also electric consumption is also negatively affected.

The heat pump has a rated heating capacity of 37.5 kW with a maximum electric absorption of 12.5 kW. The generator produces an air-flow rate of 12,000 m³/h distributed by 5 emitters uniformly distanced inside the canteen. This device was simulated by the Type 954 implemented in the TESS library. As the Scroll compressor is equipped with an inverter, simulations considered the COP variation only with source temperatures (outdoor and supply air). These data are provided by attaching an external file with the proper format to obtain in the output the real share of electric absorption under actual operating conditions. This item represents the greatest load in terms of electric consumption, as described in the following. Since the indoor environment is not equipped with a thermostat for air temperature control, the heat pump is manually activated from 09:00 to 13:00 on Monday, Wednesday and Thursday.

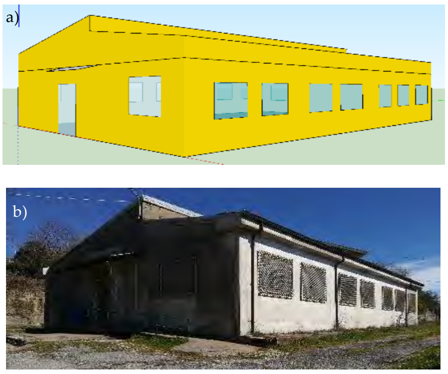

Fig. 1 – Modelled and real NE prospect of the analyzed building

Table 1 – Thickness (s), Thermal resistance (R), density (ρ) and specific heat of the vertical wall layers (U-value=0.956 W/(m²K))

	s [mm]	R [m2 K/W]	ρ [kg/m3]	c [kJ/kg K]
Plaster	15	0.017	1800	0.84
Hollow brick	250	0.513	1400	1
Air gap	50	0.179	1.2	1
Brick	120	0.150	1800	1
Plaster	15	0.017	1800	0.84

Table 2 – Thickness (s), Thermal resistance (R), density (ρ) and specific heat of the ground floor layers (U-value=1.727 W/(m²K))

	s [mm]	R [m² K/W]	ρ [kg/m³]	c [kJ/kg K]
Ceramic Tiles	10	0.01	2300	0.84
Concrete screed	60	0.103	900	1
Concrete	200	0.121	2200	1
Gravel	150	0.125	1700	0.8
Ceramic Tiles	10	0.01	2300	0.84

Table 3 – Thickness (s), Thermal resistance (R), density (ρ) and specific heat of the roof layers (U-value=1.105 W/(m²K))

	s [mm]	R [m² K/W]	ρ [kg/m³]	c [kJ/kg K]
Plaster	10	0.17	1800	0.84
Slab lightening blocks	180	0.3	1800	1
Concrete screed	60	0.103	900	1
Wooden laths	100	0.18	1800	1
Roof tiles	10	0.012	1800	0.84

2.2 Simultaneity Factor

The design of the renewable system represented by a PV generator on the grid-connected building is based on the maximization of the simultaneity factor between electric production and consumption. This parameter can be evaluated through Fig. 2, which depicts a typical situation comparing profiles concerning an electric consumption pattern (black line) and PV production (red line) on a clear day. It can be appreciated that, during the PV operation, an electric rate is directly used to satisfy the building's electrical loads (B), and another significant part (C), instead, is a surplus to share within the REC. In a monitoring campaign long "N" with data acquired every "i" timestep, the simultaneity factor can be determined by the following relation (Luthander et al., 2015):

$$SF = \frac{\sum_{i=1}^{N} B}{\sum_{i=1}^{N} (A + B)} \tag{1}$$

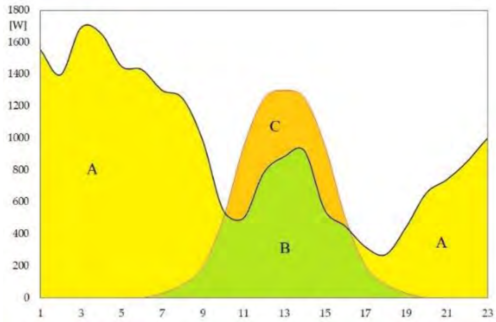

Fig. 2 – Random profiles for the simultaneity factor calculation

The TRNSYS simulations allowed us to carry out a parametric study in which the size, the type of employed PV technology and DMS were changed to identify the configuration that maximizes the result of Eq. 1, reducing the issues related to electric surpluses management. In the parametric study, three different PV technologies were considered: traditional panels equipped with mono and polycrystalline silicon cells, and another case involving tandem cells with amorphous and micro-crystalline silicon, with the main electrical features listed in Table 4, varying the installed peak powers. The favourable installation of the PV generator involves the roof pitch oriented South-West, for which an available surface of 120 m² was considered to take into account technical constraints. So, 54 mono-crystalline modules (2.19 m² each) for a maximum peak power of 24.3 kW, 60 polycrystalline modules (1.98 m² each) for a maximum peak power of 20.4 kW and 84 modules with amorphous cells (1.42 m² each) for a maximum peak power of 11.34 kW, can be potentially installed. Simulations were conducted for a year with a timestep of 1 hour by setting the present activation of the electric loads.

Table 4 – Main electric features of the considered PV panels in the parametric study

	Ppk [W]	Isc [A]	%Ppk [%/°C]	⚜REF [-]
Monocrystalline	450	11.42	-0.35	0.206
Polycrystalline	340	9.35	-0.37	0.172
◎-Si/◎c-Si	135	3.41	-0.24	0.095

In order to state the TRNSYS results' reliability, a validation procedure based on the calculation of statistical indices such as NMBE and CV-RMSE following the ASHRAE Guideline 14-2014, was carried out. These indices were calculated by Eq. 2 and Eq. 3 comparing measured (y) and simulated ($\hat{y}$) data concerning the electricity consumption for a period of one month.

$$CV(RMSE) = \frac{1}{\bar{y}}\sqrt{\frac{\sum_{i=1}^{n}(y_i - \hat{y}_i)^2}{n-p}} \quad (2)$$

$$NMBE = \frac{\sum_{i=1}^{n}(y_i - \hat{y}_i)}{(n-p)\cdot\bar{y}} \quad (3)$$

2.3 Climatic Data

The school canteen is located in Soveria Mannelli (CZ), a mountain site in South Italy characterized by 2374 HDD (Heating Degree Day). In Fig. 3, the data related to the real outdoor air humidity and temperature in the period 20/03/2024 – 20/04/2024, collected by a weather station located in the proximity of the building and employed for the building-plant model validation, are displayed. The considered days still belong to the heating period, and the huge climatic variability can be appreciated, in light of outdoor air temperatures that range between a minimum of 2.6 °C and a maximum of 27.2 °C, with an average value of 12.3 °C. In addition, the average value concerning the relative humidity is about 67%, therefore weather conditions describe a building-plant system adequately solicited from a thermal viewpoint and, consequently, this period appears suitable for the model validation. In Fig. 4, the experimental data related to horizontal solar radiation are depicted. These refer to the weather station located at the University of Calabria (with similar latitude) distinguishing between beam and diffuse components. In the TRNSYS environment, the projection on the different tilted surfaces (including the pitched roofs) was carried out by using the Reindl model. The fictitious sky temperatures, required for the calculation of the infrared exchanges of the external envelope surfaces, are not experimentally available. Therefore, in simulations, the Aubinet correlation is implemented in a specific TRNSYS Type that uses experimental values of outdoor air temperature, cloudiness factor and vapour pressure of external air. The latter was calculated starting from the monitored relative humidity and the saturation pressure corresponding to the outdoor air temperature. The glazed surfaces were selected from the software library by choosing a window with a thermal transmittance (U-value) of 2.8 W/(m²K) and a normal solar factor of $g_{\perp}$=0.70, values both close to the data of the real components. Window screens were considered never activated during the building occupation to favour daylight. Thermal losses affecting the ground floor were considered by setting the external surface with a boundary condition represented by the soil temperature. This parameter was varied to tune the building-plant model, nevertheless, the initial value was imposed equal to the site's yearly average air temperature (11.2 °C). Another parameter varied to calibrate the model is represented by the natural ventilation, which was set to 0.5 ach per hour as the initial value.

2.4 Experimental Set-Up

Different probes have been employed to monitor the parameters used for validation. A triple-phase Wi-Fi energy meter was employed to measure and collect in-cloud data concerning the building's electric consumption. The accuracy is 1% with a maximum measurement of 120 A per channel. The probe was installed near the school energy meter.

Temperature and humidity were detected by a thermo-hygrometer equipped with a Pt100 with an accuracy of ±0.1 °C and operative range -30 °C+100 °C for the temperature, and ±0.1% with an operative range of 0-100 % RH for the relative humidity.

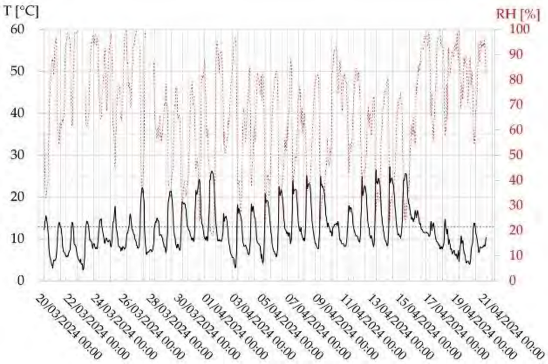

Fig. 3 – Experimental data of outdoor air temperature and humidity for the validation of the building-plant system model

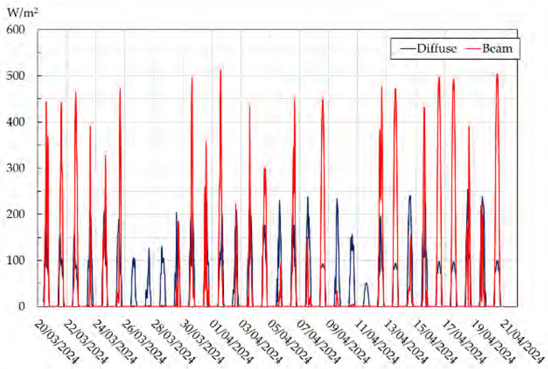

Fig. 4 – Experimental data of beam and diffuse solar irradiance on the horizontal plane used for the model validation

The global solar irradiance on the module plane is measured with a Secondary Standard Eppley Laboratory using pyranometers arranged with a spectral range of 295–2800 nm, sensitivity of 8 μV/Wm^{-2}, a 95% response time of 5 s, a non-stability and non-linearity of 0.5%, and uncertainty at an hourly average of 2%. The beam solar irradiance is measured with a CH1 pyrheliometer with a sensitivity of 10.45 μV/(Wm^{-2}), a 95% response time lower than 5 s, and a non-linearity of 0.5%.

3. Results

3.1 Model Validation

Fig. 5 shows the trends of the monitored electric consumption in the period 20/03/2024 – 20/04/2024. It can be appreciated that:

- An abrupt increase of electric consumption can be detected with the electric heat pump operation at the first switch-on in the operative days, due to the large absorbed starting power.
- The absorbed power difficulty stabilizes;
- In the period starting from Friday 05/04 and for the whole successive weekend, the heat pump was left continuously functioning because the municipality used the building for a local celebration, appreciating the power modulation due to the part-load operating mode.
- Every day, a base load of about 2300 W of absorbed electric power was detected throughout the monitored period, due to a programmed activation of a hydraulic pump for 5 hours per day (from 6:00 a.m. to 12:00 p.m.) used to supply an autoclave system connected to all the neighbouring buildings. This electric consumption is registered exclusively on the school canteen energy meter. The base electric load, represented only by artificial lighting made of LED, was neglected during simulations because very low.
- The validation was carried out in the period 05/04/2024-09/04/2024, employing climatic data (TMY) of the nearest city (Lamezia Terme), to achieve more robust results because the heat pump operated in continuous mode. After a series of several attempts, natural ventilation to 1.4 ach per hour, the temperature of the soil of 8.5 °C and a rated electric absorption of the heat pump of 10.4 kW, allowed for detecting an appreciable overlapping between the trends of simulated and experimental electric consumption (Fig. 6). The reasons for the identified setting can be explained by the high envelope air permeability, the presence of groundwater under the building and the heat pump ageing that could provide performances different from those declared by the manufacturer.

  Indeed, the heat pump was simulated with a rated COP of 3.62, lower than the declared 4.61. In the past, the heat pump was affected also by technical issues such as a loss of lowboiling fluid inside the internal units.

- The calibrated TRNSYS model simulated by a timestep of 1 hour offers an NMBE and CV-RMSE of -2.81% and 27%, respectively, in agreement with the thresholds of 10% for NMBE and 30% for CV-RMSE indicated by the ASHRAE for the calibration of a whole building simulation assuming an hourly data for one month. This result confirms that the building-plant system was properly tuned to attain reliable results even when different plant configurations are investigated in terms of electric production and consumption.

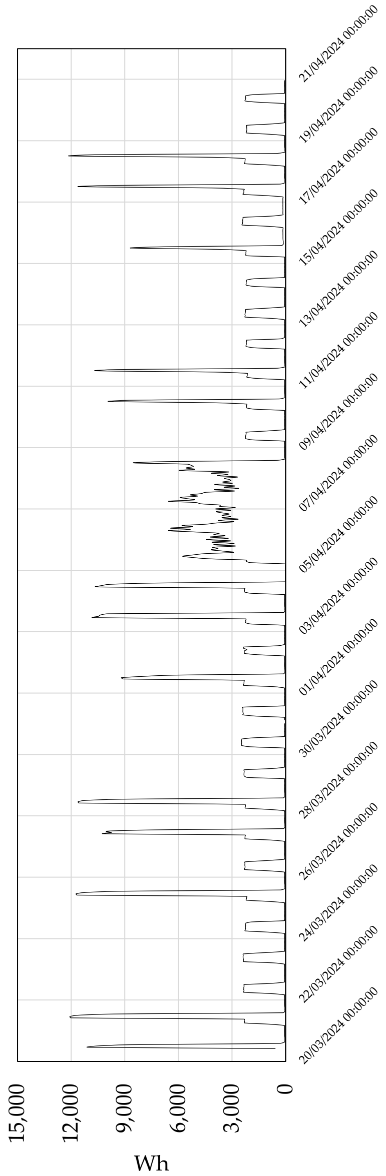

Fig. 5 – Registered electric consumptions in the monitored period

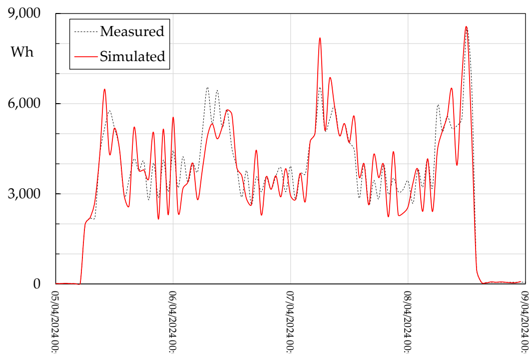

Fig. 6 – Comparison between measured and simulated electric consumptions in the period 05/04/24-09/04/24

3.2 Parametric Study

Results of the parametric study are summarized in Table 5: it is worth noting that SF increases with the installed peak power and, as expected, the mono-crystalline technology is the best choice, assuring an SF of about 70% when 24.3 kW_P (18 panels in series on 3 arrays) are installed. The polycrystalline cells are negatively affected by the lower allowable collection surface (in turn, due to the smaller electric conversion efficiency) and by the highest power temperature coefficient. The amorphous technology represents the worst choice and it appears not to be indicated to self-consume the power output. Indeed, an SF of only 14.8% was determined with the maximum installable peak power of 11.34 kW. It can be appreciated that 20 polycrystalline panels on two arrays (13.6 kW_P) produce remarkable SF (57.6%) despite the installed peak power not being so different from the maximum collection surface installable with amorphous technology.

Table 5 – Simultaneity factor as a function of PV peak power and PV technology

	P_{pk} [kW]	SF [%]
Monocrystalline	24.30	69.9%
	16.20	62.4%
	8.10	47.9%
Polycrystalline	20.40	65.5%
	13.60	57.6%
	6.80	42.5%
α-Si/μc-Si	11.34	14.8%
	7.56	8.8%
	3.78	3.0%

Fig. 7 highlights how the SF is distributed during the year for the best configuration of 24.3 kW made of monocrystalline cells. It can be appreciated that the activation of the heating plant in October paradoxically produces an abrupt drop of SF, more pronounced in November and December, when a better match between production and consumption is expected. This means that the punctual PV production does not meet the electric demands, also due to the less availability of solar irradiance. Conversely, a better situation is detected in summer as the building is not occupied by students with a corresponding decrease in electric demand and a greater probability of meeting the PV power output. The annual results presented in Table 5 benefit from the high SF value detected during the summer when the building is unoccupied. However, significant issues related to the management of electrical surplus arise in winter.

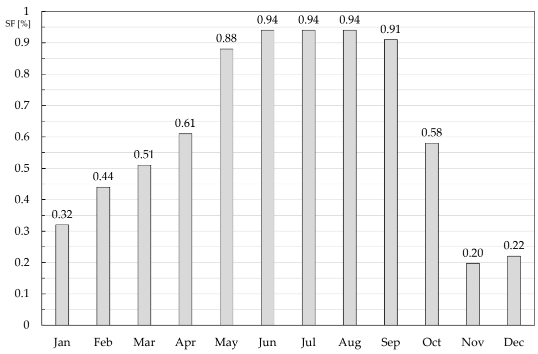

Fig. 7 – Monthly SF values with 24.3 kW of monocrystalline panels assuming the current management of electric profiles

In order to analyze the role of DSM, another simulation campaign was carried out with other functioning schedules for the heat pump and the hydraulic pump. This time, SF was determined assuming the heat pump operation from 11:00 to 15:00 (relevant to the building occupation pattern) and the hydraulic pump from 9:00 to 15:00 to synchronize solar radiation availability with electric loads. Fig. 8 shows that the new DSM produces evident improvements in winter with percentage gains ranging from 3% in March and 15% in November. In summer results remain unchanged due to the heat pump's stop. At an annual level, the forward timeshift of the electric loads produces an SF increase of more than 5 percentage points, passing from 69.9% to 75.2%. In Fig. 9 the SF monthly results are shown considering the case in which the varied DSM is combined with an accurate control of the indoor air temperature by equipping the simulated thermal zone of a thermostat operating in the band 19-21 °C. The results worsened because the control produces a limitation of the heat pump operative hours with a corresponding reduction of electric consumption. Looking at Eq. 1, this seems to produce beneficial effects due to the limitation of the rate A, although this determines also a penalization of B because the power produced cannot be self-consumed, and this aspect prevails on the first. If the thermostat assures an enhancement of the indoor comfort conditions, a simultaneous increase in PV power surplus requires to be managed within the REC. An SF enhancement is anyway detected when compared with the results depicted in Fig. 7 determining a yearly SF of 72.5%.

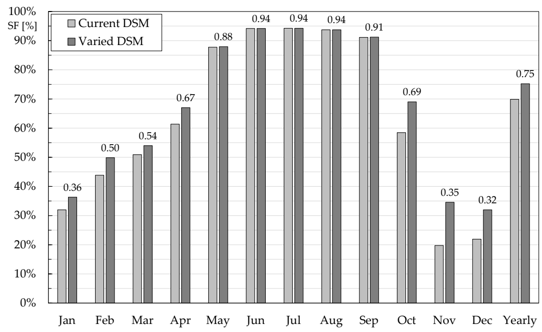

Fig. 8 – Monthly and yearly SF values with 24.3 kW of monocrystalline panels with different DSM of electric loads

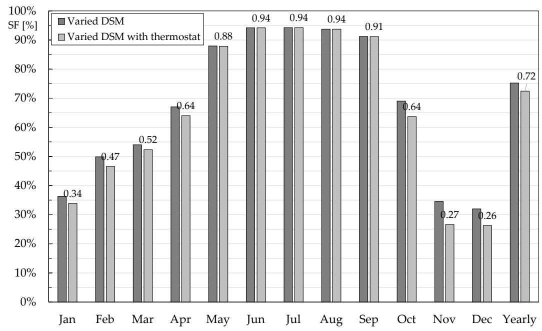

Fig. 9 – Monthly SF values with 24.3 kW of monocrystalline panels assuming a different DSM for the main electric loads

Finally, Fig. 10 depicts the SF trend with the peak power assuming mono-crystallin silicon cells with the improved DSM. It can be appreciated as a linear increment until an installed peak power of about 20 kW, successively SF increases slightly. As a consequence, the installation of greater PV powers is not recommended in front of a slight SF increase.

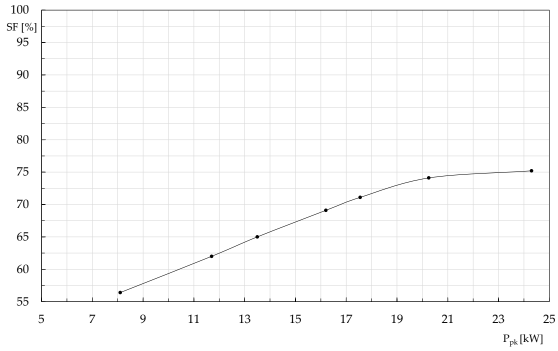

Fig. 10 – SF trend with the installed PV peak power assuming an improved DSM

4. Conclusion

A simultaneity factor between electric PV production and consumption was introduced by referring to a particular case study represented by a municipal building employed for a few hours and only 3 days per week. The simultaneity factor was calculated by varying the PV size, the PV technology and the modality of management of internal electric loads, represented prevalently by a VRF heat pump for heating and a hydraulic pump for water storage, through TRNSYS simulations. The reliability of results was achieved by a validation procedure that allowed for an NMBE and CV-RMSE of -2.8% and 27% respectively, compliant with the recommended values by ASHRAE, calculated through the comparison of simulated and experimental data collected for one month long. Results highlight how the amorphous technology is not suitable for buildings belonging to RECs due to the limited contribution given in terms of self-consumed power. Conversely, high performances can be achieved with mono-crystalline cells producing SF of about 75% when evaluated on an annual basis. This percentage is influenced positively by the limitation of the summer electric consumption due to heat pump inoperability. Despite the maximum installable peak power on roof surfaces with suitable irradiance conditions being 24.3 kW, it is not recommended to install over 20 kW because the SF augment is negligible. A significant role is given by the Demand Side Management (DSM): results showed that by shifting the device functioning toward the central hours of the day, SF increases appreciably due to better synchronism with the solar irradiance availability. The limitation of the heat pump functioning attained by a zone thermostat does not give additional improvements since the prevalent role of PV power reduction in phase with the required electric load. This study confirms that BES software can be employed profitably to assess the optimized configuration of a building-plant system involved in a local REC. This preliminary study focuses on maximizing the benefits related to identifying the optimal production-demand configuration for electricity. In subsequent studies, the results obtained will be utilized to extend the analysis to an energy community composed of multiple public and private users. This will assess whether the observations made for a single building serve as a valid methodology for the optimization of an energy community.

References

Arcuri N., Bruno R., Carpino C. 2018. "PV Driven Heat Pumps for the Electric Demand-Side Management: Experimental Results of a Demonstrative Plant". *IEEE International Conference on Environment and Electrical Engineering and IEEE Industrial and Commercial Power Systems Europe*: 1-6. https://doi.org/10.1109/EEEIC.2018.8493492

Bevilacqua P., Morabito N., Bruno R., Ferraro V., Arcuri N. 2020. "Seasonal performances of photovoltaic cooling systems in different weather conditions". *Journal of Cleaner Production* 272. https://doi.org/10.1016/j.jclepro.2020.122459

Franzoi, N.; Prada, A.; Verones, S.; Baggio, P. 2021. "Enhancing PV Self-Consumption through Energy Communities in Heating-Dominated Climates". Energies 14(14): 4165. https://doi.org/10.3390/en14144165

Heuninckx, S.; Boveldt, G.T.; Macharis, C.; Coosemans, T. 2022. "Stakeholder objectives for joining an energy community: Flemish case studies". Energy Policy 162: 112808. https://doi.org/10.1016/j.enpol.2022.112808

Lode, M.L.; Heuninckx, S.; Boveldt, G.T.; Macharis, C.; Coosemans, T. 2022. "Designing successful energy communities: A comparison of seven pilots in Europe applying the Multi-Actor Multi-Criteria Analysis". Energy Research & Social Science 90: 102671. https://doi.org/10.1016/j.erss.2022.102671

Luthander R., Widen J., Nilsson D., Palm J. 2015. "Photovoltaic self-consumption in buildings: A review". Applied Energy 142: 80-94. https://doi.org/10.1016/j.apenergy.2014.12.028

Marique, A.F.; Reiter, S. 2014. "A simplified framework to assess the feasibility of zero-energy at the neighbourhood/community scale". Energy and Buildings 82: 114–122. https://doi.org/10.1016/j.enbuild.2014.07.006

UN Environmental Program. 2024. "Global Status Report for Buildings and Construction". https://wedocs.unep.org/bitstream/handle/20.500.11822/45095/global_status_report_buildings_construction_2023.pdf?sequence=3&isAllowed=y

VV.AA. 2018. "TRNSYS 18 Reference Manual", Solar Energy Laboratory. University of Wisconsin.